

# TRACEABLE AMMONIA QUANTIFICATION AND METROLOGICAL UNCERTAINTY EVALUATION IN A SHOCK TUBE

D. Zhu<sup>1</sup>, S. Agarwal<sup>1</sup>, B. Shu<sup>1</sup>, R. Fernandes<sup>1,2</sup>, Z. Qu<sup>1</sup>

<sup>1</sup> Department of Physical Chemistry, Physikalisch-Technische Bundesanstalt, Braunschweig, Germany

<sup>2</sup> Institute of Internal Combustion Engines, Technische Universität Braunschweig, Braunschweig, Germany

E-Mail (corresponding author): denghao.zhu.ext@ptb.de; zhechao.qu@ptb.de

## Abstract:

This work emphasizes on the development of an ultra-rapid spectrally resolved tunable diode laser absorption spectroscopy (TDLAS)-based spectrometer with a scan frequency of 40 kHz for dynamic NH<sub>3</sub> quantification in a shock tube. Thanks to the high laser scan frequency, the NH<sub>3</sub> mole fraction at various stages during the dynamic process can be quantified. Besides, considering lacking metrology in shock tubes for dynamic studies, we comprehensively evaluated the uncertainty sources and budgets of thermodynamic parameters and species concentration based on *Guide to the expression of uncertainty in measurements* (GUM). The established metrological uncertainty evaluation method for shock tube experiments can be beneficial to provide traceable and high-quality data, which is vital for dynamic studies as well as chemical kinetic modelling.

**Keywords:** Ammonia; TDLAS; Shock tube; Uncertainty budget

## 1 INTRODUCTION

Ammonia is a promising zero-carbon fuel which has a comparable specific mass density to conventional fossil fuels. Compared to hydrogen, it has a 70% relatively higher specific volume density and higher boiling point, making it much easier to be liquefied and therefore significantly reducing the cost of storage and transportation. The volumetric hydrogen content of ammonia is also 70% relatively higher than hydrogen which means that ammonia is not only a good zero-carbon fuel but also a promising hydrogen carrier. A much narrower flammability limit of ammonia compared to hydrogen increases its safety property for daily usage. The “green” ammonia synthesized by

“Power-to-X” technologies ensures life-cycle carbon neutrality of using ammonia and guides to the eventual “ammonia economy” [1].

When considering ammonia as a fuel to be applied on a large scale, fundamental thermodynamic studies are required. The shock tube is one of the typical facilities that can create a quasi-instantaneously and homogeneously high-temperature and pressure environment. It is commonly used for high-temperature chemistry validation where the thermal conversion process in shock tubes can be simulated using a zero-dimensional model. To get speciation data from shock tubes, diagnostic methods are required such as laser diagnostics, mass spectrometry, or gas chromatography. Among them, tunable laser diode laser absorption spectroscopy (TDLAS) is an *in-situ*, line-of-sight, and non-invasive measurement method with high time resolution and selectivity [2]. By coupling TDLAS to shock tubes, it is able to get highly accurate time-resolved speciation data within the time scales of only several hundred microseconds to several milliseconds.

Up to now, there are limited studies on speciation measurements of ammonia and ammonia fuel blends using TDLAS in shock tubes. Alturaifi et al. [3-5] conducted several experiments by coupling TDLAS to the shock tube for NH<sub>3</sub>, N<sub>2</sub>O and H<sub>2</sub>O measurements during ammonia pyrolysis and oxidation. He and Zheng et al. [6-9] used TDLAS to measure NH<sub>3</sub>, NO, CO, CO<sub>2</sub>, H<sub>2</sub>O and temperature during ammonia and ammonia fuel blends oxidation. At PTB (National Metrology Institute of Germany), we measured the time-resolved NO profiles for pure NH<sub>3</sub> and NH<sub>3</sub>/H<sub>2</sub> fuel blends. Recently, we selected a new NH<sub>3</sub> absorption line and coupled it to the shock tube for NH<sub>3</sub> quantification [10-13].

The importance of quantifying ammonia in shock tube experiments is not only because it is the reactant, but also due to its sticky property, as well as the interest in evaluating unconsumed ammonia emissions. From the literature studies and our

previous works, there are still two concerns that are worthwhile for further investigations. Firstly, the  $\text{NH}_3$  absorption cross-sections measurements in shock tubes were all based on the assumption that an unchanged  $\text{NH}_3$  mole fraction before incident shock wave ( $T_1, P_1$ ), to immediately after reflected shock wave ( $T_5, P_5$ ). This assumption was obtained relying on the simulation results while has not been experimentally validated to our best knowledge. In our previous work, we already observed around 20%  $\text{NH}_3$  decomposition at the first spectra (at 200  $\mu\text{s}$ ) after ( $T_5, P_5$ ) at a temperature of 1933 K, therefore the cross-section measurements were limited to 1800 K. This reminds us of the importance of prerequisites for absorption cross-section measurements which merits more investigations. Secondly, there is still lacking metrological uncertainty evaluation methodology for speciation data measured in shock tubes by TDLAS although it has been used for several decades, which is particularly important in providing reliable experimental data.

Consequently, we upgraded our previous spectrometer by enhancing the scan frequency from previously 10 kHz to 40 kHz, and the corresponding data acquisition rate from 20 MS/s to 80 MS/s. The purpose is on the one hand to capture enough spectra at different stages during the dynamic process in shock tubes, especially regarding the ultra-short time duration of around 100  $\mu\text{s}$  after the incident shock wave ( $T_2, P_2$ ). On the other hand, we want to shorten the measurement time of the first spectra after the reflected shock wave ( $T_5, P_5$ ) to minimize the potential pyrolysis of  $\text{NH}_3$  at high temperatures. Based on the ultra-rapid TDLAS spectrometer, we quantified and compared the  $\text{NH}_3$  mole fractions before the incident shock wave ( $T_1, P_1$ ), after the incident shock wave ( $T_2, P_2$ ) and immediately after the reflected shock wave ( $T_5, P_5$ ) (within 25  $\mu\text{s}$ ). Also, we conducted comprehensive uncertainty evaluations on thermodynamic parameters and speciation mole fractions following

the rules of *Guide to the expression of uncertainty in measurement* (GUM) [14].

## 2 METHODOLOGY

For TDLAS, the intensity of a monochromatic continuously tunable laser source transmitted through a gaseous sample is given by the Beer-Lambert law [15]:

$$I(v) = E(t) + I_0(v) \cdot T(t) \cdot \exp[-\alpha(v)] \quad (1)$$

with the background emission  $E(t)$  at time  $t$ , initial laser intensity  $I_0(v)$ , the spectrally broadband transmission losses  $T(t)$ , and the absorbance  $\alpha(v)$ .

The absorbance spectrum  $\alpha(v)$  can be computed using the following equation:

$$\alpha(v) = -p \ln \left( \frac{I(v) - E(t)}{I_0(v) \cdot T(t)} \right) = \frac{S(T) \cdot p \cdot L \cdot g(v - v_0) \cdot x}{k_B \cdot T} \quad (2)$$

where  $S(T)$  is the absorption line strength at gas temperature  $T$ ,  $g(v - v_0)$  is the area normalized (integrated area=1) line shape function (centered at the wavenumber  $v_0$ ),  $k_B$  is the Boltzmann constant,  $p$  is the total pressure,  $x$  is the  $\text{NH}_3$  mole fraction, and  $L$  is the optical path length.

By integrating the absorbance spectrum, the  $\text{NH}_3$  mole fraction can be obtained by the following equation without the necessity to solve the line shape function.

$$A = \int \alpha(v) = \frac{S(T)_{\text{sum}} \cdot p \cdot L \cdot x}{k_B \cdot T} \quad (3)$$

## 3 EXPERIMENTAL SETUP

The schematic of the experimental setup is shown in Figure 1. The shock tube at PTB consists of a 3.5-meter driver section and a 4.5-meter driven section. The inner surface was electropolished with a diameter of 70 mm. A manometer (627F, MKS Instruments, PTB International System of Units (SI)-traceable) was installed on the top of the driven section near the diaphragm section to record the initial filling pressure. Five pressure sensors (Kistler model 603C) combined with charge amplifiers (Kistler model 5018A) were utilized for pressure measurements and shock velocity calculation.

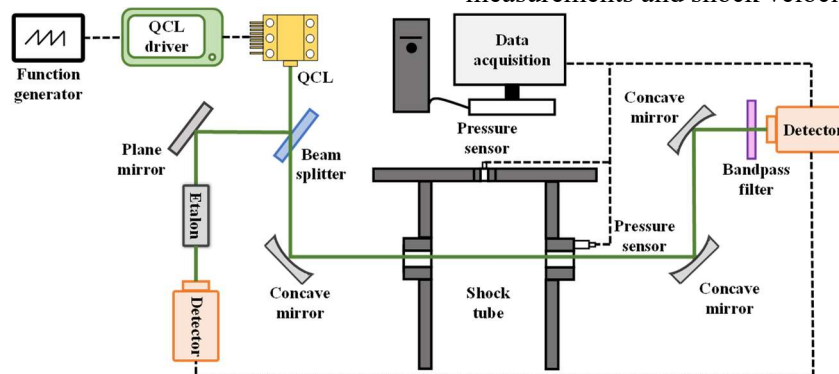


Figure 1. Schematic of the experimental setup

For laser diagnostics, two opposite  $\text{CaF}_2$  windows were installed at the same plane as the fourth pressure sensor. The mid-infrared  $\text{NH}_3$  laser

centered at  $1084.6 \text{ cm}^{-1}$  is a continuous-wave distributed-feedback quantum cascade laser (CW-DFB-QCL, Alpes Lasers). The wavelength can be

tuned from 1083 to 1089  $\text{cm}^{-1}$  by varying the current and/or temperature using a QCL driver (ITC4005QCL, Thorlabs). The laser current was modulated by a triangle-shaped ramp at a scan frequency up to 40 kHz supplied by a function generator (33500B, KEYSIGHT). From Figure 1, the laser beam was divided into two sub beams by a beam splitter (BSW711, Thorlabs). One was used to determine the dynamic laser tuning using a Germanium etalon (length 76.244 mm, traceable to PTB's length standard) before starting the measurements. The results of the etalon measurement were used to convert the x-axis of the measured spectra from the time to the wavenumbers domain. The other laser beam went through the optical windows with a path length of 7 cm via two concave mirrors (CM508-200-M01, focal length: 200 mm, Thorlabs) and was focused onto a photodetector (PVI-4TE-10, VIGO) by a concave mirror (CM508-050-M01, focal length: 50 mm, Thorlabs). A narrow bandpass filter (FB9000-500, Thorlabs) was placed in front of the detector to discriminate the signal against the background emission  $E(t)$  in Equation (1), e.g., thermal emission from the shock-heated gases. To match the ultra-

rapid scan frequency, we upgraded the acquisition system with a new DAQ card (16-bit 80 MS/s, M2p.5943-x4, Spectrum Instrumentation).

The  $\text{NH}_3/\text{Ar}$  mixtures were prepared in a 50 L stainless steel tank using high quality pure  $\text{NH}_3$  and pure Ar (HiQ 5.0, Linde). A manometer (627F, MKS Instruments, PTB SI-traceable) was installed on the top of the mixing tank to monitor the mixture pressure. Before preparing the mixtures, this tank was vacuumed overnight to a pressure below  $1 \times 10^{-7}$  mbar (TTR 91N, Leybold). When starting to prepare the mixture, a small amount of target gas first flushes the pipes twice to clean up residual gas. The mixtures were stirred by a magnetic stirrer (cyclone 300 ac, Büchiglasuster) for at least two hours to ensure homogeneity.

Table 1 shows the average mixture compositions and experimental conditions of three  $\text{NH}_3/\text{Ar}$  mixtures examined in this study. The ideal  $\text{NH}_3$  mole fraction of Mixture 1, Mixture 2, and Mixture 3 is 0.5%, 1% and 1.5%, respectively. From Table 1, it can be found that the average  $\text{NH}_3$  mole fraction is lower than the ideal value due to  $\text{NH}_3$  adsorption effect, which will be discussed later.

Table 1. Average mixture compositions and experimental conditions

Mixture	$x_{\text{NH}_3}$	$x_{\text{Ar}}$	$P_1$ /bar	$T_1$ /K	$P_2$ /bar	$T_2$ /K	$P_5$ /bar	$T_5$ /K
1	0.0037	0.9963	0.0199-0.1177	295	0.2553-0.5543	603-1200	1.1502-1.7798	988-2394
2	0.0095	0.9905			0.2563-0.5492	597-1192	1.1589-1.7643	975-2374
3	0.0137	0.9863			0.2581-0.5880	620-1195	1.1711-1.8855	1027-2380

## 4 RESULTS AND DISCUSSIONS

### a. Spectra

Figure 2 shows an exemplary pressure trace measured by the 4th pressure sensor and corresponding laser signal measured in a shock tube. The time zero is set as the arrival of the shock wave to the 5th pressure sensor. From Figure 2, two sharp pressure rises can be captured, indicating the arrival of the incident shock wave and reflected shock wave, respectively. The duration of the status ( $P_2$ ,  $T_2$ ) is quite short of around 100  $\mu\text{s}$ . To get enough spectra at ( $P_2$ ,  $T_2$ ), the scan frequency was therefore enhanced to 40 kHz, namely 25  $\mu\text{s}$  for a period. In this case, there are at least three complete spectra that can be captured. Besides, an ultra-rapid scan frequency was able to make the time duration of the first spectra at ( $P_5$ ,  $T_5$ ) as short as possible to reduce the possibility of pyrolysis at high temperature conditions.

Before starting the measurements, the etalon signal was firstly acquired to mark the relative laser wavelength. For each shot, the reference signal ( $I_0$ ) and offset signal were recorded before filling the mixture. Then the transmitted signal ( $I_t$ ) was

automatically recorded triggered by the pressure signal. By using Equation (1-2) and transferring the time-domain to wavenumber-domain using etalon signal, the spectral absorbance at different stages can be calculated. Furthermore, the concentration can be quantified by integrating the absorbance spectra using Equation (3).

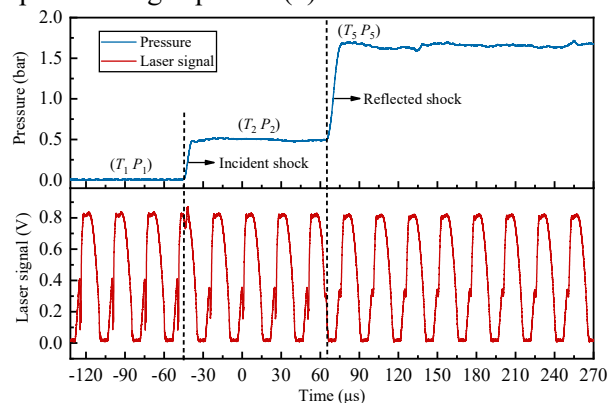


Figure 2. Exemplary pressure trace and laser signal

## b. Metrological uncertainty evaluation

Although shock tube coupled with TDLAS have been widely applied for monitoring the dynamic speciation in the past decades, the uncertainty of the measurements is commonly analysed using the root sum squared method without a standard and metrological approach [3-5]. Given this, we conducted a comprehensive uncertainty evaluation using GUM Workbench® [14]. The coverage factor is given as 1.0 throughout the uncertainty evaluations in this study. For easier illustration, we took one case from Mixture 2 ( $P_1=0.0688$  bar) as an example in the following steps.

Firstly, the heat capacity ratio of the mixture ( $\gamma$ ) before incident shock wave is calculated by Equation (4),

$$\gamma = \frac{\sum C_{p_i} x_i}{\sum C_{v_i} x_i} \quad (\text{Eq.4})$$

where  $x$  represents the mole fraction of the mixture composition;  $C_p$  and  $C_v$  represent the heat capacities at constant pressure and at constant volume, respectively.

The  $\text{NH}_3$  mole fraction before incident shock wave ( $x_{(P_1, T_1)}$ ) was calculated by Equation (3) including six relevant quantities. Specifically,  $k_B$  has a constant of  $1.380649 \times 10^{-23}$  J/K. The laser path length ( $L$ ) is 7 cm, with an uncertainty of 1.1%. The absorption spectrum is averaged over 116 scans for the ( $P_1, T_1$ ) period. The integral area of this averaged absorption spectrum ( $A_{(P_1, T_1)}$ ) is 0.0984, with an uncertainty of 1.5% which includes the uncertainty of etalon measurements. The total line intensity ( $S(T)_{(P_1, T_1)}$ ) of six transition lines at 295 K is  $8.233 \times 10^{-19}$  cm/mol, with an uncertainty of 10% from HITRAN [16]. The uncertainty of  $P_1$  is 0.0001 bar according to the calibration certificate (PTB SI-traceable). The room temperature was controlled and measured at 295 K with an uncertainty of 0.5 K. As a result,  $x_{(P_1, T_1)}$  is calculated to be 0.0101 with an uncertainty of 10.5%. Table 3 shows the uncertainty budgets of  $x_{(P_1, T_1)}$ . Clearly, the uncertainty of  $S(T)_{(P_1, T_1)}$  accounts for a significantly greater contribution (96.6%) than other quantities, which indicates an efficient way to reduce the total uncertainty by reducing the uncertainty of the line intensity.

Other quantities for heat capacity calculation were obtained from the National Institute of Standards and Technology (NIST) database. Specifically, the  $C_p$  and  $C_v$  of  $\text{NH}_3$  are 36.385 and 27.688 J/(mol·K), respectively, with an uncertainty of 0.25%. The  $C_p$  and  $C_v$  of Ar are 20.820 and 12.477 J/(mol·K), respectively, with an uncertainty of 0.15%. Overall, the heat capacity ratio  $\gamma$  of the mixture is 1.6608 with an uncertainty of 0.215%.

Secondly, the Mach number ( $M_a$ ) of the shock front is another important parameter calculated by Equation (5),

$$M_a = \frac{u_s}{\sqrt{\frac{\gamma R}{\sum M_i x_i}}} \quad (\text{Eq.5})$$

where  $u_s$  refers to the shock velocity;  $R$  is the gas constant;  $M$  is the molar mass.

The shock velocity has an uncertainty of 0.937%. The gas constant  $R$  is defined as the Avogadro constant  $N_A$  ( $6.02214076 \times 10^{23}$ ) multiplied by  $k_B$  ( $8.31446261815324$  J/(mol·K)). The molar mass of  $\text{NH}_3$  and Ar were 17.0305 and 39.948 g/mol from NIST, respectively. Overall, the Mach number is 2.332 with an uncertainty of 0.943% where the uncertainty from shock velocity contributes 97.8%. Thirdly, according to the gas dynamic equations based on one-dimensional shock wave coordinates, the pressures and temperatures ( $P_2, T_2, P_5, T_5$ ) behind the incident and reflected shock waves can be calculated by Equation (6-9).

$$P_2 = P_1 \left[ 1 + \frac{2\gamma}{\gamma+1} (M_a^2 - 1) \right] \quad (\text{Eq.6})$$

$$T_2 = T_1 \left[ 1 + \frac{2(\gamma-1)\gamma M_a^2 + 1}{(\gamma+1)^2 M_a^2} (M_a^2 - 1) \right] \quad (\text{Eq.7})$$

$$P_5 = P_1 \left[ \frac{2\gamma M_a^2 - (\gamma-1)}{\gamma+1} \right] \left[ \frac{(3\gamma-1)M_a^2 - 2(\gamma-1)}{(\gamma-1)M_a^2 + 2} \right] \quad (\text{Eq.8})$$

$$T_5 = T_1 \frac{[2(\gamma-1)M_a^2 + (3-\gamma)][(3\gamma-1)M_a^2 - 2(\gamma-1)]}{(\gamma+1)^2 M_a^2} \quad (\text{Eq.9})$$

Based on the above analysis for the heat capacity ratio and Mach number, the uncertainties of  $P_2, T_2, P_5$  and  $T_5$  can be calculated to be 2.0%, 1.35%, 2.8% and 1.8%, respectively, as shown in Table 2. Combing the uncertainties of  $P_1$  and  $T_1$ , it is evident that the uncertainties of thermodynamic parameters are increasing during the heating up process, of which the Mach number contributes the highest portion (over 90%) among all uncertainty sources.

Table 2. Uncertainty budgets of  $P_2, T_2, P_5$  and  $T_5$

Quantity	$P_1$	$T_1$	$\gamma$	$M_a$
Value	0.0688 bar	295 K	1.6608	2.332
Uncertainty (%)	0.15	0.17	0.215	0.9
$P_2$	Contribution (%)	0.6	-	0.1
	Value	<b>0.45 ± 0.008 bar (2.0%)</b>		
$T_2$	Contribution (%)	-	1.6	3.7
	Value	<b>735 ± 9.9 K (1.35%)</b>		
$P_5$	Contribution (%)	-	-	-
	Value	<b>1.636 ± 0.0458 bar (2.8%)</b>		
$T_5$	Contribution (%)	-	0.9	5.0
	Value	<b>94.1</b>		

	Value	<b>1328 ± 23.9 K (1.8%)</b>
--	-------	-----------------------------

The NH<sub>3</sub> mole fraction at ( $P_2$ ,  $T_2$ ) and ( $P_5$ ,  $T_5$ ) can be calculated by Equation (3), the same method as for  $x_{(P_1, T_1)}$ . However, except for Boltzmann constant and path length, the values and uncertainties of the rest quantities have changed. As mentioned above, with an ultra-rapid scan frequency of 40 kHz, three complete spectra at ( $P_2$ ,  $T_2$ ) can be recorded and averaged. The area  $A_{(P_2, T_2)}$  of the averaged absorbance is 0.0907 with an uncertainty of 1.5%. The line intensity at ( $P_2$ ,  $T_2$ ) is reduced to  $3.098 \times 10^{-19}$  cm/mol with an uncertainty of 10%. In a consequence, the NH<sub>3</sub> mole fraction at ( $P_2$ ,  $T_2$ ) is 0.0094 with an uncertainty of 10.5%.

To quantify the NH<sub>3</sub> mole fraction immediately after the reflected shock wave, we only used the first spectral absorbance to minimize the effect of

possible pyrolysis with the growing time, especially for high temperature cases. With this ultra-rapid scan frequency, the largest time interval between the first scan and reflected shock wave is less than 25  $\mu$ s, basically within 12.5  $\mu$ s as only the first half period of the scan was considered. The line intensity at ( $P_5$ ,  $T_5$ ) is further reduced to  $6.902 \times 10^{-20}$  cm/mol with an uncertainty of 10%. As a result, the integrated absorbance  $A_{(P_5, T_5)}$  is only about a half value compared to that at ( $P_1$ ,  $T_1$ ) or ( $P_2$ ,  $T_2$ ), leading to a larger uncertainty of 2%. Resultantly, the NH<sub>3</sub> mole fraction immediately after the reflected shock wave  $x_{(P_5, T_5)}$  is 0.0099 with an uncertainty of 11%, which is 0.5% larger than that of  $x_{(P_1, T_1)}$  and  $x_{(P_2, T_2)}$  owing to a higher uncertainty in pressure, temperature, and integrated absorbance.

Table 3. Uncertainty budgets of NH<sub>3</sub> mole fraction at different stages

Quantity	$k_B$	$L$	$A_{(P_1, T_1)}$	$S(T)_{(P_1, T_1)}$	$P_1$	$T_1$	
Value	$1.380649 \times 10^{-23}$ J/K	7 cm	0.0984	$8.233 \times 10^{-19}$ cm/mol	0.0688 bar	295 K	
Uncertainty (%)	-	1.1	1.5	10	0.15	0.17	
$x_{(P_1, T_1)}$	Contribution (%)	-	1.1	2.1	96.6	0.1	0.1
	Value	<b>0.0101 ± 0.0011 (10.5%)</b>					
Quantity	$k_B$	$L$	$A_{(P_2, T_2)}$	$S(T)_{(P_2, T_2)}$	$P_2$	$T_2$	
Value	$1.380649 \times 10^{-23}$ J/K	7 cm	0.0907	$3.098 \times 10^{-19}$ cm/mol	0.45 bar	735 K	
Uncertainty (%)	-	1.1	1.5	10	2.0	1.4	
$x_{(P_2, T_2)}$	Contribution (%)	-	1.1	2.0	91.7	3.6	1.6
	Value	<b>0.0094 ± 0.0010 (10.5%)</b>					
Quantity	$k_B$	$L$	$A_{(P_5, T_5)}$	$S(T)_{(P_5, T_5)}$	$P_5$	$T_5$	
Value	$1.380649 \times 10^{-23}$ J/K	7 cm	0.0427	$6.902 \times 10^{-20}$ cm/mol	1.636 bar	1328 K	
Uncertainty (%)	-	1.1	2	10	2.8	1.8	
$x_{(P_5, T_5)}$	Contribution (%)	-	1.0	3.4	86.3	6.6	2.7
	Value	<b>0.0099 ± 0.0011 (11%)</b>					

### c. Ammonia quantification

The NH<sub>3</sub> mole fraction and corresponding uncertainties at ( $T_1$ ,  $P_1$ ), ( $T_2$ ,  $P_2$ ) and immediately after ( $T_5$ ,  $P_5$ ) of all cases for Mixture 1-3 are calculated by Equation (3), as shown in Figure 3. The dashed lines indicate the ideal mole fraction for mixture preparation. From Figure 3, when taking the measurement uncertainties into consideration, no evident NH<sub>3</sub> mole fraction variation can be observed, indicating no evident pyrolysis occurs during this dynamic process. Besides, it is concentration independent as three mixtures show consistent results. Note that this conclusion is only valid for the NH<sub>3</sub> mole fraction of the first spectra measured after the reflected shock wave, a time interval of less than 25  $\mu$ s. As the time grows, the pyrolysis process will happen at such high  $T_5$ . Nevertheless, this study restricts the valid conditions of the assumption for cross-section measurements, especially for high temperatures. From Figure 3, another consistent phenomenon for three mixtures is that with the increase of  $P_1$ , the

NH<sub>3</sub> mole fraction increases and then levels off when  $P_1$  is larger than 0.06 bar. This result strongly indicates that at lower  $P_1$ , the relative NH<sub>3</sub> loss is larger. Especially for a low mole fraction mixture (e.g. Mixture 1), the largest relative NH<sub>3</sub> loss can be over 50% at the minimum  $P_1$ .

Note that before each experiment, we have used the same mixture as the experimental one to passivate the inner surface of the shock tube. Nonetheless, it is far from enough especially for low  $P_1$  and low initial mole fraction mixtures. Some studies also used a specific higher concentration mixture as a compensation of NH<sub>3</sub> adsorption. However, this method also brings a risk that the NH<sub>3</sub> mole fraction after passivation is even higher than the target value. Up to now, there is still lacking golden standard passivation method for NH<sub>3</sub> studies in shock tubes. The difficulty is that the passivation process has a random nature, and highly depends on the initial pressure, mixture mole fraction, inner surface materials, passivation times, passivation time duration, vacuuming pumps and procedures. In

addition, the loss could also happen during the mixture preparation as  $\text{NH}_3$  will also adsorb to the inner surface of the mixing tank, and it is quite difficult to monitor this process. Therefore, at least for low  $\text{NH}_3$  mole fraction mixture and low  $P_1$  conditions, it is strongly recommended to quantify the initial  $\text{NH}_3$  mole fraction. A key quantity for thermodynamic parameters calculation, as well as an important input for modelling studies.

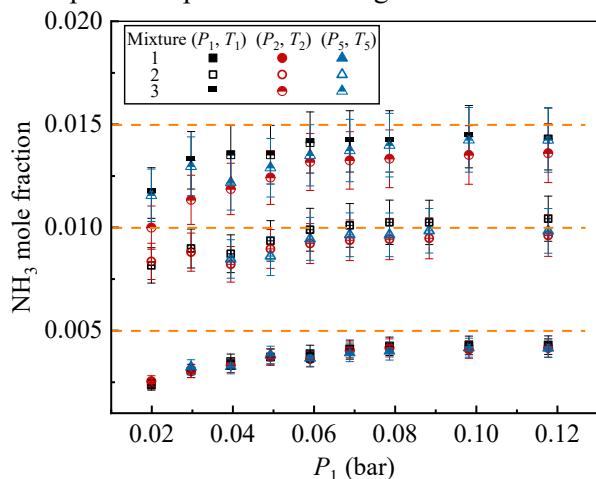


Figure 3.  $\text{NH}_3$  mole fraction at  $(T_1, P_1)$ ,  $(T_2, P_2)$  and immediately after  $(T_5, P_5)$  of Mixture 1-3

## 5 SUMMARY

We developed an ultra-rapid TDLAS spectrometer (40 kHz scan frequency) and quantified the ammonia mole fraction before the incident shock wave ( $P_1, T_1$ ), after the incident shock wave ( $P_2, T_2$ ), and immediately after the reflected shock wave ( $P_5, T_5$ ) (within 25  $\mu\text{s}$ ). No significant variation in  $\text{NH}_3$  mole fraction was observed during the shock tube experiments, indicating no evident  $\text{NH}_3$  pyrolysis during this dynamic process. This restricts the valid conditions for cross-section measurements. Additionally, we compared the  $\text{NH}_3$  mole fraction at different  $P_1$  values and found that  $\text{NH}_3$  loss occurred, even with a passivation procedure, at lower  $P_1$  ( $<0.06$  bar in this study). For low  $\text{NH}_3$  mole fraction mixtures, the largest relative  $\text{NH}_3$  loss exceeded 50% at the minimum  $P_1$  of 0.02 bar (ideally 0.5%  $\text{NH}_3$  in the mixture). Therefore, it is strongly recommended to quantify the initial  $\text{NH}_3$  mole fraction during shock tube experiments via an online *in situ* method, particularly for low  $\text{NH}_3$  mole fraction mixtures and low  $P_1$  conditions.

The uncertainties of thermodynamic parameters and the mole fraction of speciation measured by TDLAS in shock tubes have been metrologically evaluated. For the current study, the uncertainties of  $P_2, T_2, P_5$  and  $T_5$  are 2.0%, 1.35%, 2.8% and 1.8%, respectively. The uncertainties of  $\text{NH}_3$  mole fraction at  $(P_1, T_1)$ ,  $(P_2, T_2)$ , and immediately after  $(P_5, T_5)$  based on integrated absorbance are 10.5%, 10.5%

and 11%, respectively. This methodology provides an insight into the uncertainty budgets of each quantity and can be generalized to other similar studies.

## 6 REFERENCES

- M. Li, D. Zhu, X. He, K. Moshhammer, R. Fernandes, B. Shu, Experimental and kinetic modeling study on auto-ignition properties of ammonia/ethanol blends at intermediate temperatures and high pressures, *Proc. Combust. Inst.* 39 (2022) 511-519.
- R.K. Hanson, D.F. Davidson, Recent advances in laser absorption and shock tube methods for studies of combustion chemistry, *Prog. Energy Combust. Sci.* 44 (2014) 103-114.
- S.A. Alturaifi, O. Mathieu, E. L. Petersen, An experimental and modeling study of ammonia pyrolysis, *Combust. Flame.* 235 (2022) 111694.
- S.A. Alturaifi, O. Mathieu, E. L. Petersen, Shock-tube laser absorption measurements of  $\text{N}_2\text{O}$  time histories during ammonia oxidation, *Fuel Commun.* 10 (2022) 100050.
- S.A. Alturaifi, O. Mathieu, E.L. Petersen, A shock-tube study of  $\text{NH}_3$  and  $\text{NH}_3/\text{H}_2$  oxidation using laser absorption of  $\text{NH}_3$  and  $\text{H}_2\text{O}$ , *Proc. Combust. Inst.* 39 (2022) 233-241.
- D. He, D. Zheng, Y. Du, J. Li, Y. Ding, Z. Peng, Laser-absorption-spectroscopy-based temperature and  $\text{NH}_3$ -concentration time-history measurements during the oxidation processes of the shock-heated reacting  $\text{NH}_3/\text{H}_2$  mixtures, *Combust. Flame.* 245 (2022) 112349.
- D. Zheng, D. He, Y. Du, Y. Ding, Z. Peng, Shock tube study of the interaction between ammonia and nitric oxide at high temperatures using laser absorption spectroscopy, *Proc. Combust. Inst.* 39 (2022) 4365-4375.
- D. Zheng, D. He, Y. Du, Y. Ding, Z. Peng, Nitromethane as a nitric oxide precursor for studying high-temperature interactions between ammonia and nitric oxide in a shock tube, *Combust. Flame.* 250 (2023) 112644.
- D. Zheng, D. He, Y. Du, J. Li, M. Zhang, Y. Ding, Z. Peng, Experimental study of the methane/hydrogen/ammonia and ethylene/ammonia oxidation: Multi-parameter measurements using a shock tube combined with laser absorption spectroscopy, *Combust. Flame.* 254 (2023) 112830.
- D. Zhu, Z. Qu, M. Li, S. Agarwal, R. Fernandes, B. Shu, Investigation on the NO formation of ammonia oxidation in a shock tube applying tunable diode laser absorption spectroscopy, *Combust. Flame.* 246 (2022) 112389.
- D. Zhu, L. Ruwe, S. Schmitt, B. Shu, K. Kohse-Höinghaus, A. Lucassen, Interactions in Ammonia and Hydrogen Oxidation Examined in a Flow Reactor and a Shock Tube, *J. Phys. Chem. A* 127 (2023) 2351-2366.
- S. Agarwal, L. Seifert, D. Zhu, B. Shu, R. Fernandes, Z. Qu, Investigations on Pressure Broadening Coefficients of NO Lines in the  $1\leftarrow 0$  Band for  $\text{N}_2, \text{CO}_2, \text{Ar}, \text{H}_2, \text{O}_2$  and He, *Appl. Sci.* 13 (2023).

- D. Zhu, S. Agarwal, L. Seifert, B. Shu, R. Fernandes, Z. Qu, TDLAS spectrometer for the measurements of absorption cross-sections and absolute quantification of ammonia for dynamic processes at elevated temperature and pressure, *Analyst* (under review).
- BIPM/ISO: Guide to the Expression of Uncertainty in Measurement, International Organization for Standardization, 1995, ISBN 92-67-20188-3.
- Z. Qu, O. Werhahn, V. Ebert, Thermal Boundary Layer Effects on Line-of-Sight Tunable Diode Laser Absorption Spectroscopy (TDLAS) Gas Concentration Measurements, *Appl. Spectrosc.* 6 (2018) 853-862.
- I. E. Gordon, L. S. Rothman, R. J. Hargreaves, R. Hashemi, E. V. Karlovets, F. M. Skinner, E. K. Conway, C. Hill, R. V. Kochanov and Y. Tan, et al., The HITRAN2020 molecular spectroscopic database, *J. Quant. Spectrosc. Radiat. Transf.* 277 (2022) 107949.